J Sol-Gel Sci Technol (2016) 78:166–170
DOI 10.1007/s10971-015-3916-9

ORIGINAL PAPER: SOL-GEL AND HYBRID MATERIALS FOR DIELECTRIC, ELECTRONIC, MAGNETIC AND FERROELECTRIC APPLICATIONS

Effect of doping concentration and annealing temperature on threshold voltages of bipolar resistive switching in Mn-doped $BiFeO_3$ films

Jinming Luo[1] · Haining Zhang[1] · Jianping Wen[1] · Xiaodong Yang[1]

Received: 21 August 2015 / Accepted: 12 November 2015 / Published online: 9 December 2015

Abstract Nonvolatile bipolar resistive switching has been investigated in Mn-doped $BiFeO_3$ thin films fabricated by sol–gel method. Based on the analyses of X-ray diffractometer and X-ray photoelectron spectroscopy, the threshold voltages for forming and set operations in bipolar resistive switching, which are found to depend on Mn doping concentration and annealing temperature, can be ascribed to the variation of oxygen vacancy concentration and grain size. Therefore, the modulated ionic oxygen vacancy conductivity has been suggested to play a pivotal role in the resistive switching of Mn-doped $BiFeO_3$ thin films.

Graphical Abstract The forming and set voltages of resistive switching depend on doping concentration and annealing temperature.

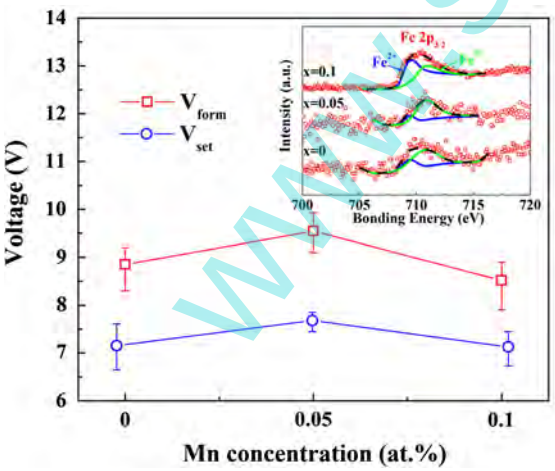

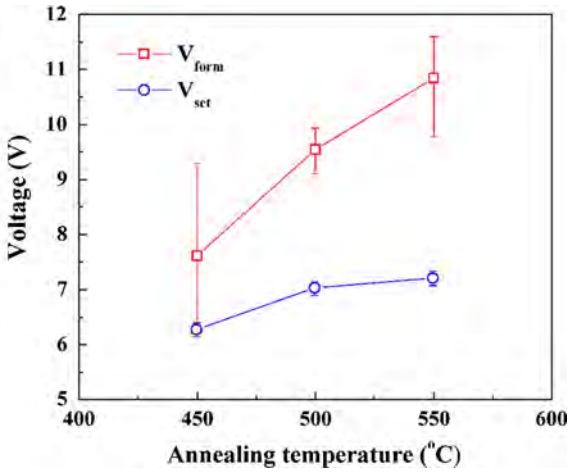

✉ Jinming Luo
zsuljm@163.com

[1] School of Physics and Optical Information Sciences, Jiaying University, Meizhou 514015, Guangdong, People's Republic of China

Keywords Threshold voltages · Resistive switching · Bismuth ferrite · Thin films · Sol–gel

1 Introduction

In the past few years, ferroelectrics have been extensively investigated as promising solid-state memories [1, 2]. Bismuth ferrite (BFO), one of the most important ferroelectrics, has attracted considerable attention due to its multiferroic properties [3–5]. Recently, resistive switching (RS) controlled by external voltages has been reported in BFO-based thin films [6–10], showing good potential in future resistance random access memories (RRAM). From an application perspective, the study of RS mechanism is of key technological importance.

Conceivable mechanisms have been invoked to account for the RS phenomenon in BFO-based thin films in the literature. Shuai et al. [8] attributed the observed interface-

related RS characteristic to an electric field-induced carrier trapping and detrapping effect, which changes the depletion layer thickness at the Au/BFO interface. Yang et al. [9] reported an electronic conductor–insulator transition in Ca-doped BFO thin films which was interpreted in terms of the modulated electronic conduction caused by the variation of oxygen vacancy (OV) distribution under voltage bias. Yin et al. [10] also concluded that the redistribution of OVs in grain boundaries could play an important role in the RS of the polycrystalline pure BFO films. Although the migration/diffusion of OVs is believed to be responsible for the RS behavior in BFO-based thin films, the underlying physical origin remains elusive, and further related investigations would be essential. In this article, Mn is used as a doping element due to the advantageous electric, magnetic and resistive switching properties in BFO thin films [11–14]. The effect of doping concentration and annealing temperature on threshold voltages of bipolar resistive switching (BRS) has been studied in $BiFe_xMn_{1-x}O_3$ (BFMO) thin films prepared by chemical solution deposition, and a better understanding of the modulated ionic conductivity of OVs has been promoted to interpret the dependence of threshold voltages on Mn doping concentration (x) and annealing temperature.

2 Experimental

BFMO ($x = 0$, 0.05, 0.1) thin films were deposited on commercial Pt/Ti/SiO_2/Si substrates by sol–gel method. The precursor solutions were prepared using 99 % $Bi(NO_3)_3{\cdot}5H_2O$ (3.09 g for $x = 0$, 0.05, 0.1), 99 % $Fe(NO_3)_3{\cdot}9H_2O$ (2.45 g for $x = 0$, 2.33 g for $x = 0.05$, 2.20 g for $x = 0.1$) and 99 % $C_6H_9MnO_6{\cdot}2H_2O$ (0.08 g for $x = 0.05$, 0.16 g for $x = 0.1$) with 99.5 % acetic acid (10 ml) and 99 % ethylene glycol monomethyl ether (20 ml) as the mixed solutions, where excess $Bi(NO_3)_3{\cdot}5H_2O$ (5 mol%) has been added to compensate the Bi loss during the annealing process. The final concentration of the precursor was 0.2 mol/L. Then the BFMO thin films were deposited by spin coating at 3000 rpm for 30 s and dried at 350 °C for 5 min in air. This process was repeated several times until the desired film thickness of about 350 nm was attained, and then the films were annealed in air atmosphere for 30 min at 450, 500 and 550 °C.

The crystalline structures of BFMO thin films were examined by a Rigaku X-ray diffractometer (XRD, D-MAX 2200 VPC) in θ–2θ mode with Cu Kα radiation ($\lambda = 0.154$ nm), and the microstructures of films were characterized by a scanning probe microscope (SPM, CSPM5500). The chemical states of Fe ions in the films were investigated by X-ray photoelectron spectroscopy (XPS, ESCALAB 250). After Pt top electrode deposition on the films with a diameter of 0.3 mm, the current–voltage characteristics were measured at room temperature with a Keithley 4200 semiconductor characterization system in voltage scanning mode.

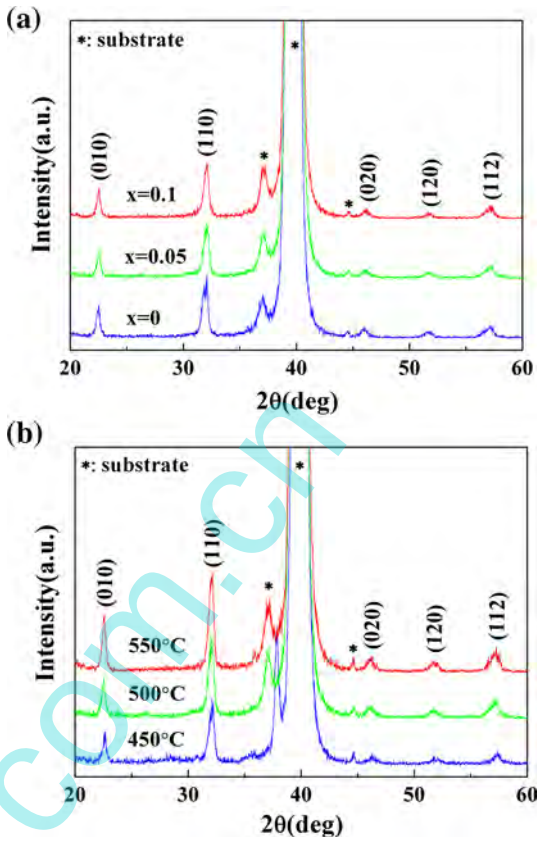

Fig. 1 (*Color online*) XRD patterns with different **a** Mn doping concentrations and **b** annealing temperatures in BFMO thin films

3 Results and discussion

The XRD patterns of BFMO thin films grown on Pt/Ti/SiO_2/Si substrates with different Mn-doped concentrations and annealing temperatures are demonstrated in Fig. 1a, b. All these films with a perovskite structure are obtained, and no other secondary phases are observed within the XRD detection limit. The average grain size of thin films can be estimated according to the Scherrer equation:

$$D = 0.89\frac{\lambda}{\beta\cos\theta} \quad (1)$$

where D is the average grain size, λ is the X-ray wavelength, β is the full width at half-maximum (FWHM) of peaks and θ is the Bragg angle. From Fig. 1a, the average grain sizes of Mn-substituted ($x = 0$, 0.05, 0.1) BFO films are calculated to be about 24.93, 24.66 and 24.59 nm, respectively, suggesting that there is little change in grain

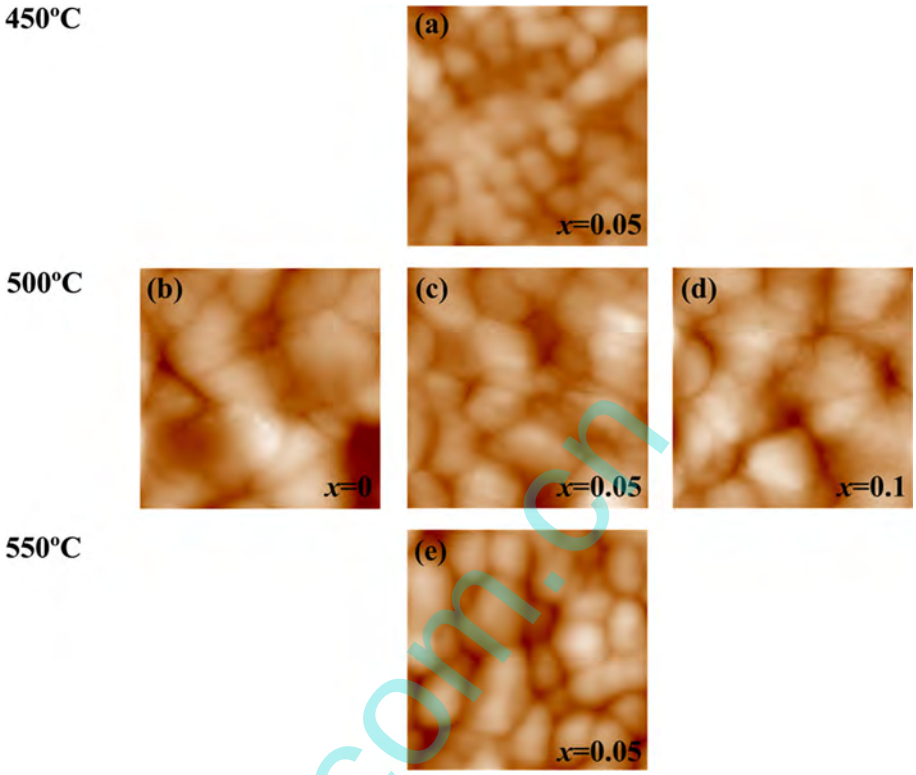

Fig. 2 (*Color online*) SPM images of BFMO thin films annealed at **a** 450 °C, **b**–**d** 500 °C and **e** 550 °C with different Mn doping concentrations (x). All of the image areas are 600 × 600 nm^2

size with Mn substitution due to the similar ionic radii between Mn and Fe atoms and the high substitution tolerance of Mn atoms in BFO films [11]. Additionally, when increasing annealing temperature, the intensity of XRD peaks gets stronger and the average grain size of $BiFe_{0.95}Mn_{0.05}O_3$ thin films becomes larger as described in Fig. 1b. The calculated grain sizes are about 23.14 nm at 450 °C, 24.66 nm at 500 °C and 25.5 nm at 550 °C, which is indicative of an improvement in crystalline quality. Figure 2 shows the corresponding SPM images of the BFMO thin films. As seen, with Mn substitution (Fig. 2b–d), no evident difference of the film surface and the average grain size can be observed, whereas with increasing annealing temperature (Fig. 2a, c, e), the average grain size of $BiFe_{0.95}Mn_{0.05}O_3$ thin films increases and the crystallinity improves as well, which is consistent with the XRD results.

The typical BRS characteristic of Pt/$BiFe_{0.95}Mn_{0.05}O_3$/Pt memory devices annealed at 500 °C has been discussed as an example in Fig. 3a, where the arrows represent the direction of sweep voltage. To activate the memory device, a forming process is required by applying a high negative voltage (V_{form}) and compliance current of 5 mA on Pt top electrodes, which is shown in the inset of Fig. 3a. After that, the current–voltage curves of BRS have been measured. With the negative voltage increasing, the current rapidly increases at a critical voltage (V_{set}) and the device switches from high resistive state (HRS) to low resistive state (LRS), which is called a "set." When an appropriate positive voltage is applied, the current suddenly drops to a low value and the device switches back from LRS to HRS, which is called a "reset." This BRS behavior can be repeatedly observed on application of the opposite voltage polarities. Furthermore, double-logarithmic current–voltage curves are replotted in Fig. 3b at the negative voltage sweep region, where the inset shows the positive region. The green lines demonstrate the fitting results of current conduction. In LRS, the current conduction follows Ohmic law, corresponding to the conductivity of memory devices, while in HRS, a typical space-charge-limited current (SCLC) conduction is observed. According to SCLC conduction, in the low-voltage regions, the current–voltage curve on log–log scale shows an Ohmic behavior (slope ~ 1). As voltage increases, the current conduction transitions from Ohmic to Child's law (slope ~ 2). This conduction mechanism suggests that the OVs could be of major importance during the resistance switching in Pt/BFMO/Pt devices.

In order to reveal the role of OVs in BRS, we measured the current–voltage characteristics by varying the Mn doping concentration and recorded the threshold voltages for forming (V_{form}) and set (V_{set}) operations obtained by this experiment. Figure 4 shows the relationship between the threshold voltages and the Mn doping content, and both V_{form} and V_{set} exhibit the similar behavior. With 5 % Mn substitution, the threshold voltages are higher than that in

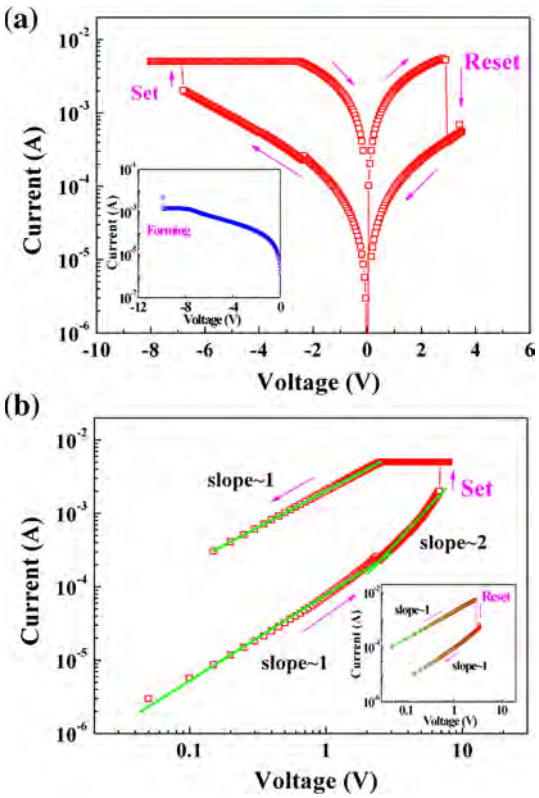

Fig. 3 (*Color online*) BRS characteristics in $Pt/BiFe_{0.95}Mn_{0.05}O_3/Pt$ devices. **a** The typical current–voltage behavior of BRS plotted in semi-log scale. The *inset* shows the forming process. **b** The current–voltage curves replotted on a log–log scale at the negative sweep voltage region, with the *inset* showing the positive region

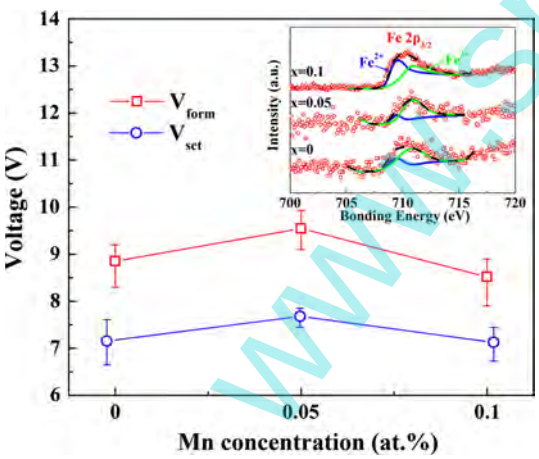

Fig. 4 (*Color online*) Threshold voltages for forming and set with absolute values. The *inset* shows XPS spectra of Fe $2p_{3/2}$ depending on Mn doping concentration in BFMO thin films

pure BFO, whereas when the amount of the Mn dopant increases to 10 %, the lower threshold voltages can be observed. To elucidate this phenomenon, XPS is used to confirm the variation of OV concentration in the thin films. As shown in the inset of Fig. 4, the positions of Fe $2p_{3/2}$ are

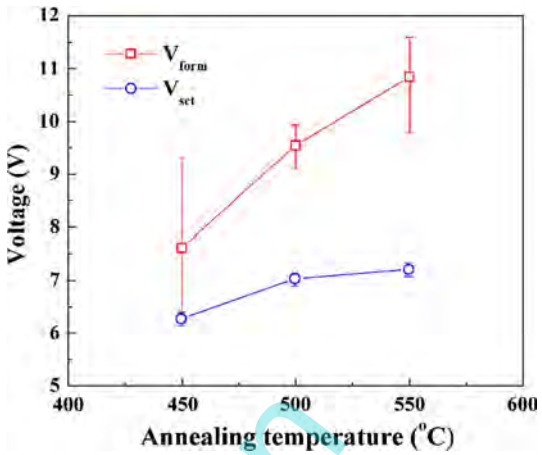

Fig. 5 (*Color online*) Annealing temperature dependence of the threshold voltages with absolute values in BFMO thin films

expected to be at 709.4 eV for Fe^{2+} and 710.7 eV for Fe^{3+}, respectively [13]. From the fitting results, compared with pure BFO thin films, the content of Fe^{2+} in 5 % Mn-substituted BFO films decreases, indicating that a small amount of Mn substitution could reduce the number of OVs and suppress the formation of Fe^{2+}. However, in 10 % Mn-substituted BFO films, the content of Fe^{2+} increases, suggesting that a large amount of Mn substitution could increase the number of OVs and accelerate the formation of Fe^{2+} [15].

To further demonstrate the characteristic of OVs, the current–voltage measurements of BRS have also been taken in $BiFe_{0.95}Mn_{0.05}O_3$ thin films annealed at different temperatures. As illustrated in Fig. 5, it can be found that the threshold voltages are dependent on annealing temperature. When the annealing temperature increases from 450 to 550 °C, the forming voltage increases significantly and shows large fluctuation at 450 °C which could be owing to the more random ordering of OVs along the large number of crystalline grains at lower annealing temperature. Meanwhile, the set voltage exhibits a slight change with the annealing temperature. The detailed discussion will be devoted hereinafter.

According to the preceding conductive filament mechanism [13, 14], the forming process corresponding to the formation of filament can be accomplished by the migration/diffusion of OVs through the thin film under an external voltage, while the subsequent switching process corresponding to the rupture/recovery of filament is supposed to take place at a localized region rather than at a bulk region in the thin film. This may be the reason for V_{set} showing weak dependence on both Mn doping concentration and annealing temperature. Yang et al. [9] have investigated the RS characteristic in Ca-doped BFO films and believed that the ionic conductivity of OVs plays a key role for determining the threshold voltages of BRS in BFO-

based thin films. The ionic conductivity of OVs can be effectively modulated by the OV concentration depending on the Mn substitution at room temperature. When increasing the concentration, the ionic conductivity is enhanced, facilitating the formation of conducting filament which is originated from the OVs through nanoionic transport process, leading to the reduction in the threshold voltages. On the contrary, while decreasing the concentration, the ionic conductivity is reduced and the higher threshold voltages are attainable. Thus, without regard to the grain size effect due to the little change of grain size, the varying Mn doping contents give different effects on the OV concentration as well as the ionic conductivity in the film, resulting in the variation of the threshold voltages as shown in Fig. 4. However, when increasing the annealing temperature, not only the concentration of OVs changes [10, 16], but also the average grain size of thin films varies. Considering that it is difficult to know whether the ionic current is through the grain volumes or through the grain boundaries in polycrystalline BFO-based thin films, the grain size effect on the ionic conductivity and the threshold voltages would be quite complicated, leading to the different results between the observation in Fig. 5 and that in other literature [17].

4 Conclusions

In summary, BRS characteristics with Mn doping concentration and annealing temperature have been investigated in Pt/BFMO/Pt sandwiched devices. The XRD results demonstrate that the average grain size of films increases with annealing temperature but shows little change with Mn doping. Based on the result as well as the XPS, the modulated ionic oxygen vacancy conductivity has been presented to be responsible for the variation of threshold voltages for forming and set operations with the Mn doping concentration and annealing temperature.

Acknowledgments This work was supported by the Natural Science Foundation of Guangdong Province (No. 2014A030310410) and the Research Foundation from Department of Education of Guangdong Province (No. 314B0109). The author greatly acknowledges Prof. B. Wang and Prof. Y. Zheng (Sun Yat-Sen University) for valuable suggestions and discussions.

References

1. Chen WJ, Zheng Y, Wang B (2014) Pinning effects of dislocations on vortex domain structure in ferroelectric nanodots. Appl Phys Lett 104(22):222912
2. Wu CM, Chen WJ, Zheng Y, Ma DC, Wang B, Liu JY, Woo CH (2014) Controllability of vortex domain structure in ferroelectric nanodot: fruitful domain patterns and transformation paths. Sci Rep 4:3946
3. Kuang DH, Tang P, Yang SH, Zhang YL (2015) Effect of annealing temperatures on the structure and leakage mechanisms of $BiFeO_3$ thin films prepared by the sol–gel method. J Sol-Gel Sci Technol 73(2):410–416
4. Ghafoor I, Siddiqi SA, Shahid Atiq S, Riaz S, Naseem S (2015) Sol–gel synthesis and investigation of structural, electrical and magnetic properties of Pb doped $La_{0.1}Bi_{0.9}FeO_3$ multiferroics. J Sol-Gel Sci Technol 74(2):352–356
5. Kim JW, Raghavan CM, Kim SS (2015) Structural and electrical properties of $0.7BiFeO_3$–$0.3CaTiO_3$ solid solution thin films deposited from solutions. J Sol-Gel Sci Technol 76(3):693–698
6. Luo JM, Chen SH, Bu SL, Wen JP (2014) Resistive switching and Schottky diode-like behaviors in Pt/$BiFeO_3$/ITO devices. J Alloys Compd 601:100–103
7. Kim WH, Son JY, Jang HM (2014) Confinement of ferroelectric domain-wall motion at artificially formed conducting-nanofilaments in epitaxial $BiFeO_3$ thin films. ACS Appl Mater Interfaces 6(9):6346–6350
8. Shuai Y, Zhou S, Bürger D, Helm M, Schmidt H (2011) Nonvolatile bipolar resistive switching in Au/$BiFeO_3$/Pt. J Appl Phys 109(12):124117
9. Yang CH, Seidel J, Kim SY, Rossen PB, Yu P, Gajek M, Chu YH, Martin LW, Holcomb MB, He Q, Maksymovych P, Balke N, Kalinin SV, Baddorf AP, Basu SR, Scullin ML, Ramesh R (2009) Electric modulation of conduction in multiferroic Ca-doped $BiFeO_3$ films. Nat Mater 8(6):485–493
10. Yin K, Li M, Liu Y, He C, Zhuge F, Chen B, Lu W, Pan X, Li RW (2010) Resistance switching in polycrystalline $BiFeO_3$ thin films. Appl Phys Lett 97(4):042101
11. Huang JZ, Wang Y, Lin Y, Li M, Nan CW (2009) Effect of Mn doping on electric and magnetic properties of $BiFeO_3$ thin films by chemical solution deposition. J Appl Phys 106(6):063911
12. Riaz S, Shah SMH, Akbar A, Atiq S, Naseem S (2015) Effect of Mn doping on structural, dielectric and magnetic properties of $BiFeO_3$ thin films. J Sol-Gel Sci Technol 74(2):329–339
13. Luo JM, Lin SP, Zheng Y, Wang B (2012) Nonpolar resistive switching in Mn-doped $BiFeO_3$ thin films by chemical solution deposition. Appl Phys Lett 101(6):062902
14. Luo JM, Chen RQ, Lin SP (2014) The physical nature of bipolar resistive switching in Pt/$BiFe_{0.95}Mn_{0.05}O_3$/Pt memory devices. Phys Status Solidi A 211(1):191–194
15. Qi X, Dho J, Tomov R, Blamire MG, MacManus-Driscoll JL (2005) Greatly reduced leakage current and conduction mechanism in aliovalent-ion-doped $BiFeO_3$. Appl Phys Lett 86(6):062903
16. Chen X, Zhang H, Ruan K, Shi W (2012) Annealing effect on the bipolar resistive switching behaviors of $BiFeO_3$ thin films on $LaNiO_3$-buffered Si substrates. J Alloys Compd 529:108–112
17. Zhu X, Zhuge F, Li M, Yin K, Liu Y, Zuo Z, Chen B, Li RW (2011) Microstructure dependence of leakage and resistive switching behaviours in Ce-doped $BiFeO_3$ thin films. J Phys D Appl Phys 44(41):415104